6

Single Shot Diagnostics of Quasi-Continuously Pumped Picosecond Lasers Using Fast Photodiode and Digital Oscilloscope

Michal Jelínek, Václav Kubeček and Miroslav Čech
Czech Technical University in Prague
Czech Republic

1. Introduction

Ultrashort laser pulses with duration in the range between 10 and 100 ps play important role in many applications, such as microsurgery, micromachining, laser ranging, nonlinear optics etc. Methods enabling precise measurement of such pulses duration are therefore essential. Common silicon photodiodes used in combination with ordinary oscilloscopes cannot be used for such a precise measurement because of low temporal resolution of the whole system. Therefore, several sophisticated methods based on optical or electro-optical effects were developed in the past decades and are still widely used (Diels, 1995; Keller, 2007; Rulliere, 2003). The first method based on nonlinear optical effect is measurement of second order autocorrelation function of the measured light pulse. This function is always symmetric and does allow to obtain detailed information on the exact pulse shape and pulse duration is calculated assuming the certain pulse temporal profile. This method, which can be used either for single or repetitive pulses, is in principle very precise but has also several disadvantages. The whole measuring system has to be aligned precisely and the measured beam has to enter the system in accurately aligned angle. Precision depends also on control of the delay line used for scanning autocorrelation measurement. Because the resulting pulse length is in this case calculated from many points, it is clear that it represents average value of the real pulses lengths and is difficult to evaluate pulse duration stability or study some other effects, i.e. pulse shortening under specific conditions. The single shot autocorrelators on the other hand can measure the autocorrelation function from only single laser shot but exact interpretation is not also unique. The only direct picosecond pulses measurement method based on electro optical effect uses a streak camera. This method allows to measure single pulse duration and shape but several consecutive pulses in the pulse train cannot be measured with sufficient temporal resolution. It is also necessary to carefully align whole measuring system and perform its rigorous calibration including readout.

Repetitive signals as mode locked pulse trains from continuously pumped lasers can be measured using sampling oscilloscopes in combination with fast detectors enabling resolution in units of picoseconds. For signals with repetition rates below several kHz sampling oscilloscopes cannot be used and only real time oscilloscopes with lower resolution are available. In the past few years fast real time oscilloscopes with analog bandwidth up to

40 GHz primarily designed for digital signal processing became available. In combination with sufficiently fast photodiode (commercially available with bandwidth up to $\sim 60\,\text{GHz}$) a powerful tool for single ultrashort laser pulse characterization appeared. The photodiode - oscilloscope system for measurement of such laser pulses has several advantages. This procedure is simple to perform because the laser beam can be easily directed on the photodiode and very precise alignment of the measuring system is not necessary. The measurement is also repeatable, quick, and moreover duration of several pulses in the train can be recorded simultaneously from the single laser shot which enables investigation of special effects, such as pulse shortening in the laser output pulse train (Kubecek, 2009). Furthermore, oscilloscopes offer sophisticated functions and e.g. pulse duration statistics from thousands of pulses can be studied.

The subject of this chapter is theoretical and experimental study of the diagnostics of picosecond laser single pulses and pulse trains with repetition rates below 100 Hz using measuring system consisting of a fast real time oscilloscope and InGaAs PIN photodiode. In the first section physics of detection and general properties of photodiodes are described. In the second section theoretical analysis of pulse duration measurement method using oscilloscope - photodiode system is performed. Measuring system impulse response based on calculation from the corresponding datasheet parameters is discussed and subsequently resulting value is calculated for the given system. The third section deals with experimental verification of the described measurement method and calculated impulse response. Three laboratory laser systems based on neodymium (Nd) doped active materials and operated in quasi-continuously pumped regime were studied. The lasers were passively mode-locked by the semiconductor saturable absorbers and generated output trains consisted of 5 to 100 pulses. For some measurements single pulse was extracted. The pulses had duration in the range between 10 and 200 ps depending on the laser system. The pulse duration was measured simultaneously by our oscilloscope - photodiode system and at least one of precise optical measuring system (autocorrelator or streak camera) to investigate how short pulses can be measured with sufficient accuracy. Subsequently, it was possible to use the measuring system not only for instantaneous estimation of duration of the pulse shorter than corresponding impulse response, but moreover to investigate pulse duration stability using oscilloscope sophisticated statistics functions. In addition, two tested laser systems were operated under special regime resulting in pulse duration shortening along the output pulse train, which was possible to study precisely at each individual laser shot.

2. Physics of detection and photodiodes

Photodiodes represent one of fundamental light detection devices and play almost un-substitutable role in many applications, where the time and amplitude characteristic of the incoming light pulses has to be investigated or further exploited. Among the main advantages of photodiodes belong ease of use, fast time response, sensitivity at sufficiently wide spectral region, reasonably low thermal and electrical noise, and small dimensions enabling integration in electro-optics devices. Photodiodes are mostly used for detection of laser light pulses in many applications, such as telecommunications, sensing, security, and laser systems monitoring.

Light detection by a semiconductor material is based on the well-known phenomena of photon absorption (Saleh, 2007). If the incident photon energy exceeds the band gap energy of the semiconductor, an electron-hole pair is released. These charge carriers move by diffusion to places with lower concentration and may contribute to electrical current, if the semiconductor is connected into some electrical circuit. Since the diffusion rate is slow, these photo-conductors cannot be used as sufficiently fast photodetectors.

The situation changes when a photodiode formed by PN junction is used. Between the P and N regions, there is a depletion layer consisted of positively and negatively charged fixed ions. These ions form electrical field in the direction from N to P. If the photon is absorbed in this depletion layer, the electrons and holes are accelerated by the described electrical field. In this layer the carriers move by drift process which depends on the electrical field and is much quicker than diffusion. The depletion layer can be further extended applying reverse bias voltage on the photodiode which significantly decreases the carrier transit time. Reverse bias voltage (below the breakdown threshold) increases the noise component formed by dark current. In relation to the detector speed, capacitance formed by the depletion layer has to be treated and kept as low as possible, because it significantly contributes to the overall capacitance of the detector therefore influences its RC constant. Depletion layer capacitance is proportional to its area and inversely proportional to its thickness. Because the area relates to the photodiode responsivity, there has to be a trade-off between these values and fast photodiodes have lower sensitivity.

In order to extend the depletion layer, the intrinsic-doped layer can be inserted between P and N regions forming PIN diode. This leads to reduction of the necessary reverse bias voltage to several volts and simultaneously to rise the detector speed because most of photons are absorbed in this layer and generated carriers drift through this layer accelerated by the bias voltage. Furthermore, thicker depletion layer decreases the junction capacitance.

In the following section photodiode parameters with emphasis on the spectral region and response time will be discussed from the point of material and construction parameters. Requested spectral region ranging approximately from 500 to 1500 nm and covers the most of wavelengths used in solid state lasers enabling ultrashort pulses generation. Spectral region of the photodiode is mainly limited by its material parameter - the absorption layer band gap. As the photon absorption does not occur when the incident photon energy is less than absorption layer band gap E_g, the long-wavelength component λ_{cutoff} is limited by $\lambda_{cutoff} = hc/E_g \Rightarrow \lambda_{cutoff}$ [μm] = 1.24/E_g [eV]. Therefore, common silicon (Si) photodiodes can be used for wavelengths only up to $\sim 1.1\,\mu$m. There is also second well-known semiconductor-compound material - gallium arsenide (GaAs). In the pure form, its long-wavelength region is limited to about 850 nm. By adding other component, the wavelength region can be significantly extended. Usage of many compounds has been published but in the commercially available photodiodes mainly Indium (In) component is used in the discussed spectral region. Pure InAs has λ_{cutoff} of about 3.4 μm and depending on its concentration in $In_xGa_{1-x}As$ compound, the wavelength range can be tuned. Mainly used compound has $x \sim 0.5$ determining λ_{cutoff} of $\sim 1.7\,\mu$m (Bitter, 2000).

Usage of GaAs-based material for the PIN photodiode construction has also other advantage in the charge carrier mobility. The electron mobility in GaAs is about five times higher than in Si while the hole mobility is comparable (Gibbons, 1987). As for construction parameters, it has already been said that in order to obtain fast response time it is necessary to keep the depletion layer capacitance as low as possible. Because of the mentioned reasons commercially available photodiodes based on GaAs / InGaAs have higher frequency bandwidth in comparison with the silicon photodiodes. The fastest photodiodes for telecommunication have to be based on InGaAs because of its desirable spectral response around 1.5 μm.

Besides these standard-type PIN photodiodes there is an extensive effort on the new photodiodes concepts development and utilization mainly in the telecomunication technique. Novel high-speed and high-power photodiodes with bandwith higher than 100 GHz were demonstrated. These new configurations are aimed to overcome the main disadvantages of the classical PIN photodiodes.

The bandwidth-efficiency and saturation current of the photodiode can be improved using the Dual-Depletion Region (DDR) detector (Effenberger, 1996). The depletion region of this structure consists of a InGaAs absorption layer and a InP drift (buffer) layer. This leads to the reduction of the junction capacitance due to increased depletion layer thickness. Moreover, the electrons must travel across both InGaAs and InP layers, whereas much slower holes must travel only across the InGaAs layer resulting in equalization of the transit times for electrons and holes.

Improved approach is the Uni-Travelling Carrier (UTC) photodiode (Ishibashi, 2000; Nagatsuma, 2011). This device utilizes only electrons as the active carriers. The active region consists of a p-InGaAs absorption layer and a wideband i-type carrier-collection layer. Photo-generated minority electrons diffuse from the absorption layer to the depleted collection layer, where they are accelerated and transported to the contact. A diffusion barrier made in the p-InGaAs layer prevents the electrons from diffusing into the p-contact while the generated holes can diffuse to the contact material. The photo-response is therefore determined by the electron diffusion time in the absorption layer which can be very thin leading to high bandwidth. Furthermore, the output peak current increases linearly with increasing input energy, and the waveform does not significantly change until it reaches the saturation point. In comparison with the waveform of the PIN photodiode, which consists from two current components (initial fast component attributed to electron transport and the slow tail caused by hole transport).

In order to increase the quantum efficiency of the standard (vertically-illuminated) PIN photodiode, which depends on the absorption layer thickness, a waveguide detection scheme was used, where the light absorption is perpendicular to current collection (Malyshev, 2004). Using this scheme it is possible to achieve high absorption efficiency and high speed simultaneously due to the decoupling of the efficiency from the absorption layer thickness. Efficient operation of these photodiodes based on the thin film germanium on silicon was successfully demonstrated (Wang, 2008).

Another approach leading to high-speed photodetectors is based on the metal-semiconductor Schottky junction, mainly developed in the MSM (Metal-Semiconductor-Metal) photodiode (Berger, 1996; Kache, 2005). Its structure is comprised of back-to-back Schottky diodes that use an interdigitated electrode configuration on the top of the active absorbing layer. This construction leads to low capacitance in comparison with the standard PIN photodiodes and therefore the MSM photodiode response speed is mostly limited by the transit time of the photo-generated carriers. Different materials may serve as the active layer and besides IR and visible spectral range also UV detectors were demonstrated successfully (Liu, 2010).

3. Picosecond pulse measurement using oscilloscope - photodiode system

3.1 Measuring system response

This chapter is aimed at measurement of ultrashort light pulses with duration between 10 and 200 ps generated by mode-locked lasers. The measurement is performed using oscilloscope - photodiode system and therefore overall response time of these both components has to be treated. Response time of each electrical component is limited by its electrical frequency bandwidth which is usually defined at the frequency where a sinusoidal output signal amplitude is attenuated to about 70 % of its original value (or in other terms the signal power is attenuated to 50 %), also known as -3 dB point. Let's consider the pulse width (duration) as full width at half maxima (FWHM) of light intensity. For the pulse width measurement the laser pulse shape can be in good approximation considered as Gaussian and therefore sum of square calculation of the real pulse duration $FWHM_{REAL}$ can be used:

$$FWHM_{REAL} = \sqrt{FWHM_{MEAS}^2 - FWHM_{SYSTEM}^2} \tag{1}$$

where $FWHM_{MEAS}$ is measured pulse width and $FWHM_{SYSTEM}$ is the minimal pulse width (impulse response or response to a Dirac delta function) of the measuring system. This instrumental constant can be calculated as

$$FWHM_{SYSTEM} = \sqrt{FWHM_{OSC}^2 + FWHM_{PD}^2} \tag{2}$$

where $FWHM_{OSC}$ is the oscilloscope minimal pulse width (given by the oscilloscope impulse response) and $FWHM_{PD}$ is the photodiode minimal pulse width. Into this calculation also influence of cables and connectors can be included when their frequency bandwidth cannot be neglected in comparison with other measuring components bandwidth. Similar theorem can be used for the calculation of rise time (RT) as the system response on the step input signal (Johnson, 1993; Keller, 2007).

3.2 Minimal pulse width and rise time of the measuring system components

Minimal pulse width FWHM and rise time RT of the measuring components can be calculated for the given frequency bandwidth f_{3dB} according to the formulas

$$FWHM = \frac{K_{FWHM}}{f_{3dB}}, \; RT = \frac{K_{RT}}{f_{3dB}} \tag{3}$$

Constant K varies in range from 0.3 to 0.5 according to the step or impulse response and also according to calculation performed for the oscilloscope or photodiode.

3.2.1 Photodiode response

The photodiode rise time can be calculated for the given electrical bandwidth using $K_{RT} = 0.35$. This value is based on the RC element step response and derived for example in (Johnson, 1993; Keller, 2002). It is also accepted by most of photodiode manufacturers who state rise time value in datasheets according to this calculation. The photodiode impulse response can be calculated using $K_{FWHM} = 0.312$ which is also derived in (Keller, 2002) and assumes the Gaussian response.

3.2.2 Oscilloscope response

Calculation of the oscilloscope response is little bit more complicated because the constant K relates to the oscilloscope type. Generally, two types of oscilloscopes are distinguished according to their shape of frequency response. Analog oscilloscopes and digital oscilloscopes with 3 dB bandwidth less than 1 GHz usually have Gaussian frequency response. This type of frequency response slowly decreases towards -3 dB attenuation and further. For this type of oscilloscopes is possible to use similar constants as for the photodiode. However, fast digital oscilloscopes with higher bandwidth have maximally flat or so-called brick wall response. In this type the frequency response is much flatter below defined -3 dB frequency but then drops rapidly. These oscilloscopes have several advantages. Signals with frequencies below f_{3dB} can be measured more precisely and higher frequency signals do not produce sampling alias errors. However, for this type of oscilloscope the assumptions and formulas for the Gaussian pulse are not valid precisely. Also the K_{RT} value is higher and ranging from 0.4 to 0.5 (Agilent, 2011; Tektronix, 2009). The K_{FWHM} is not precisely defined and according to uncertainty of K_{RT} its value can be just estimated.

3.2.3 Calculation of the measuring system impulse response

According to the previous analysis, the step and impulse response of the measuring system used in our experiments can be calculated. The measuring system consisted of the PIN photodiode EOT ET-3500 (EOT, 2011) connected by high frequency SMA cable to the real time oscilloscope LeCroy SDA-9000 (LeCroy, 2009) [1]. Datasheet parameters of the photodiode are as following: cutoff frequency >15 GHz, rise and fall time <25 ps, spectral range 1000 - 1650 nm, responsivity 0.88 A/W @ 1550 nm, active area diameter 32 μm, junction capacitance 0.12 pF. Important datasheet parameters as well as rise time and minimal pulse width calculation are summarized in Table 1.

Compo-nents & System	Datasheet values		Step response	Impulse response			
	f_{3dB} [GHz]	RT [ps]	RT [ps]	K_{FWHM}	FWHM [ps]	K_{FWHM}	FWHM [ps]
LeCroy	9.0	<49	49	0.44	49	0.40	45
EOT	15.0	<25	25	0.31	21	0.31	21
System	-	-	55	-	53	-	50

Table 1. Datasheet values and calculated system response $FWHM_{SYSTEM}$.

The system rise time can be calculated directly from the given datasheet values. The minimal pulse width is calculated from the given frequency bandwidth. For the oscilloscopes two values of K_{FWHM} are used. The first value of 0.44 is the same as used for the step response calculation, the second value of 0.4 is the estimation based on fact that the impulse response for the Gaussian systems is about 0.9 times shorter than step response (Andrews, 1989). It can be seen that the calculated minimal FWHM given by the impulse response is about 50 ps.

[1] Trade names are used to specify the experimental setup only.

4. Experimental investigation of picosecond laser pulses

4.1 Experimental determination of the measuring system minimal FWHM

Minimal FWHM was determined experimentally using an experimental fiber laser generating mode-locked pulses at 1.5 μm with duration less than 2 ps (measured by the autocorrelator). Pulse of this duration can be assumed as Dirac delta function for our measuring system. In order to avoid nonlinearities in the photodiode and oscilloscope, during all the measurements the oscilloscope vertical resolution was set at 5 mV/div and the signal amplitude was about 20 mV. The oscilloscope bandwidth was set to maximal analogue bandwidth of 9 GHz with the sampling frequency of 40 GS/sec. The oscilloscope enables two regimes of waveform acquisition and display - linear (only measured points are displayed) and *sin(x)/x* (approximation by this function). It was experimentally found that the FWHM measurement difference using these two acquisition regimes is about 1 ps and can be neglected. Therefore, most of further described measurements were performed in the linear acquisition regime.

There are two possibilities how to determine the FWHM of the measured pulse. The first is use of build-in function of the oscilloscope - Width at 50 %. The oscilloscope also enables to show histogram or statistics of these measured values. The second possibility is to save the data and perform a curve fit by Gaussian function. It has been found that using a Gaussian fit is for our pulses adequate and the determined FWHM of a such pulse with duration below 80 ps is about 18 % shorter than the value measured by the oscilloscope. Because of this uncertainty, most of FWHM values presented below were determined by the Gaussian fit of the measured pulse shape. All the presented values represent average value of about 100 pulses.

Recorded pulse from the 1.5 μm fiber laser with duration of 2 ps using *sin(x)/x* waveform approximation is shown in Fig. 1. The width measured by the oscilloscope was 75.5 $\pm$ 1.5 ps.

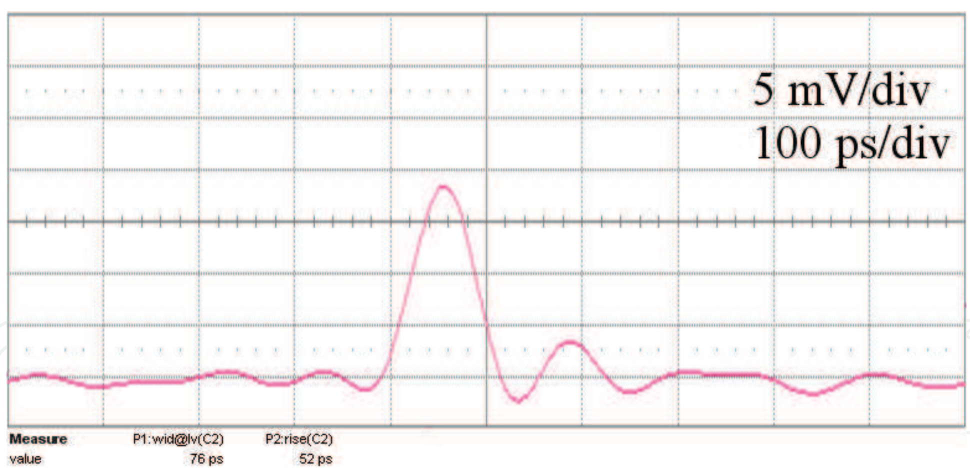

Fig. 1. Oscilloscope trace of the measured 2 ps long pulse using *sin(x)/x* approximation.

In Fig. 2 similar pulse recorded in the linear acquisition regime is shown. The width measured by the oscilloscope was 76 $\pm$ 2 ps. According to the Gaussian fit the pulse width was 63 $\pm$ 2 ps. There is a difference of about 13 ps in comparison with theoretically calculated minimal FWHM of $\sim$ 50 ps given in Table 1 which can be explained by uncertainity of used constants K, datasheet values, and influence of the cable and connectors.

There is also the second possibility to determine the FWHM_{SYSTEM} using the longer pulse with known duration FWHM_{REAL} and from the measured FWHM_{MEAS} to calculate the

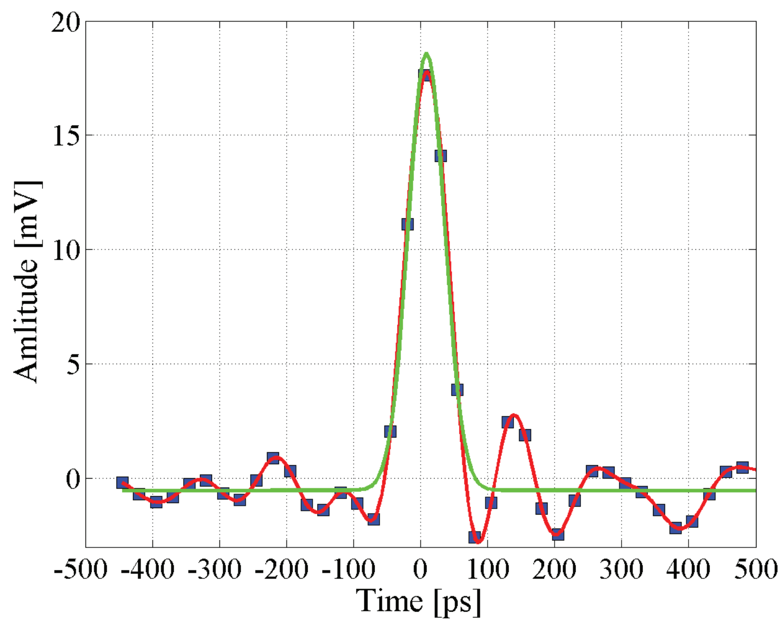

Fig. 2. Measured 2 ps long pulse (dots) and its Gaussian fit (green line) and Spline fit (red curve).

system response. In our experiments we have used a laboratory designed mode-locked Nd:YAG laser providing stable 22 ± 2 ps pulses (measured by the streak camera and autocorrelator) with repetition rate of 10 Hz at the wavelength of 1.06 μm (Jelinek, 2011; Kubecek, 2011). The laser system schematic is shown in Fig. 3. From the Gaussian fit of the measured pulse the width of 64 ± 2 ps was determined and using this value the $FWHM_{SYSTEM}$ of 60 ps was calculated. This value is in good agreement with experimentally determined value of 63 ps obtained using fiber laser.

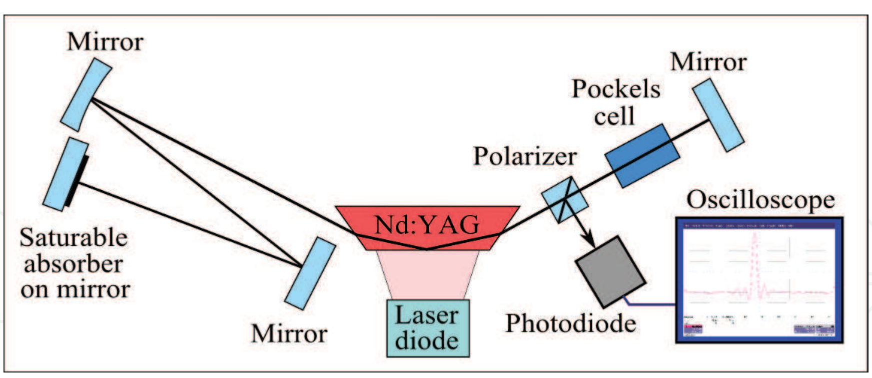

Fig. 3. Schematic of the Nd:YAG laser system generating 22 ± 2 ps pulses.

4.2 Duration estimation of pulses shorter than system impulse response time

In order to determine how short pulses can be reliably measured using our calibrated measuring system, pulses generated by two other passively mode-locked laser sources were measured and the real pulse width was calculated using both constants $FWHM_{SYSTEM}$. The first source was continuously pumped and mode locked Nd:YAG laser generating pulses in range of 17 to 21 ps (measured by the autocorrelator) with repetition rate of 110 MHz. The second source was quasi-continuously pumped and mode-locked Nd:GdVO$_4$ laser generating after cavity dumping from the Q-switched trains single pulses with duration of 56 ps (measured by the autocorrelator and streak camera) at the repetition rate of 30 Hz (Kubecek, 2010). Calculated pulse widths are shown in Table 2 and also in Fig. 4 together with calibration curves for both FWHM$_{SYSTEM}$ constants.

Laser	Pulse width FWHM [ps]				
	Measured real (autocorrelator or streak)	LeCroy value	Gaussian approximation (our value)	Calculated value for FWHM$_{SYSTEM}$: 60 ps	63 ps
Er fiber CW ML[2]	2	76 ± 2	63 ± 2	19 ± 7	-
Nd:YAG SP ML[2]	22 ± 2	79 ± 2	64 ± 2	22 ± 5	11 ± 8
Nd:YAG CW ML[2]	17 - 21	79 ± 2	66 ± 3	27 ± 7	20 ± 9
Nd:GdVO$_4$ SP ML[2]	56 ± 8	90 ± 6	82 ± 12	56 ± 16	52 ± 18

Table 2. Measured and calculated pulse widths for all studied laser sources.

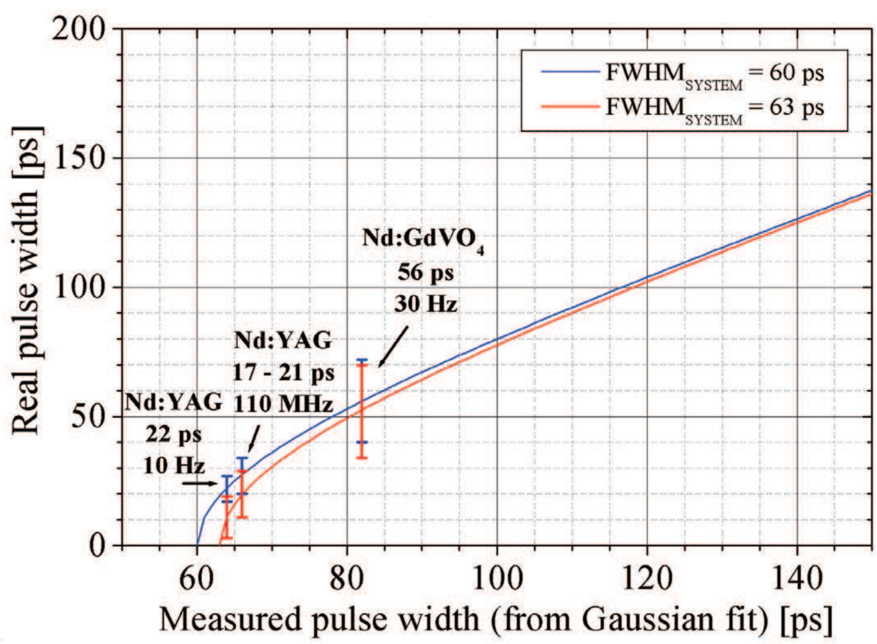

Fig. 4. Calibration curves for our measuring photodiode-oscilloscope system (for FWHM$_{SYSTEM}$ of 60 and 63 ps) and calculated real pulse durations of three measured laser sources

It can be seen that the real pulse width calculation from the measured $\sim$20 ps pulses is possible, but error up to 50 % may be introduced according to FWHM$_{SYSTEM}$ constant choice and the uncertainty of the measurement and the Gaussian fit. The real pulse width calculation for $\sim$50 ps pulses is more realistic and for both calibration curves (for different FWHM$_{SYSTEM}$ constants) does not introduce significant error. The uncertainty originates mainly from the laser stability itself.

[2] ML: mode-locking, CW: continuous wave, SP: single pulse

4.3 Single pulse duration stability investigation

The oscilloscope - photodiode system can be used for the single pulse duration stability investigation. An example of such measurement is shown in Fig. 5. Duration of the single pulses from the mode-locked Nd:$GdVO_4$ laser was measured using oscilloscope's build-in function and histogram from ~2000 successive pulses was shown. In spite of the fact that using the oscilloscope - photodiode system there may be some uncertainty in the absolute pulse width calculation, the width stability from many pulses can studied.

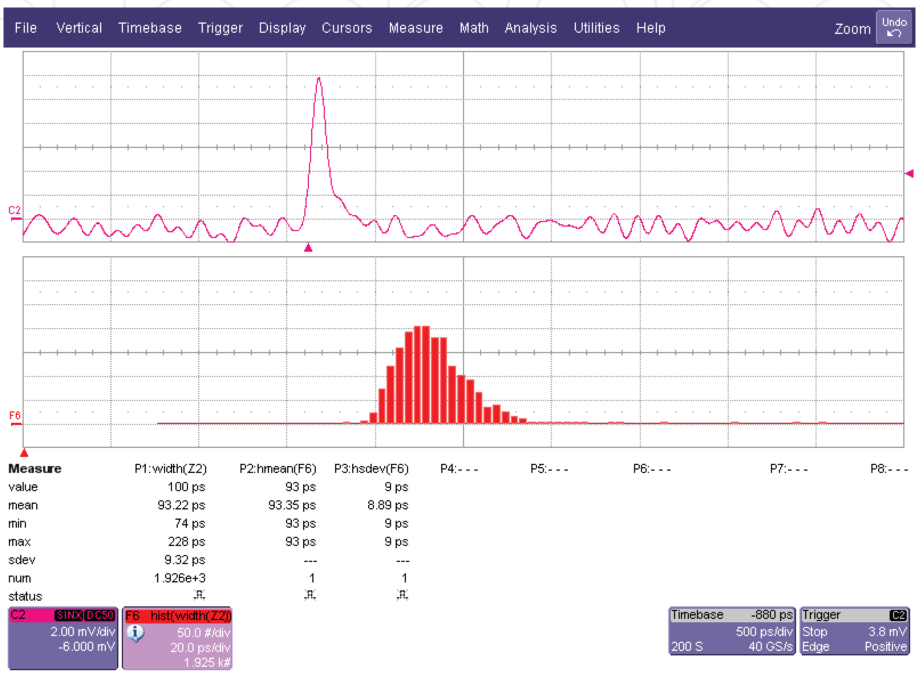

Fig. 5. Single pulse stability investigation using the oscilloscope statistical functions. Upper trace: measured pulse, lower trace: pulse width histogram from ~2000 successive pulses.

4.4 Investigation of the pulse shortening along the Q-switched mode-locked train

Using the oscilloscope - photodiode system it is possible to measure not only the temporal and energetic stability of the single pulses, but moreover to study some special effects, such as pulse width shortening along the laser output train containing tens to hundreds of pulses. Investigation of such effect in single output train cannot be performed by available optical measuring methods. As it was mentioned in the previous chapter, in spite of the fact that using the oscilloscope - photodiode system there may be uncertainty in the absolute pulse width, the pulse shortening effect studied in two pulsed laser systems can be clearly observed. The first laser system was based on Nd:$GdVO_4$ active material and passively mode locked by the semiconductor saturable absorber. The active medium was quasi-continuously pumped by the laser diode at repetition rate of 30 Hz. The 30 μJ laser output pulse train consisted of 12 pulses and its oscillogram is shown in Fig. 6. Lower traces show details of the highest pulse - pulse no. 3 in the train and later pulse no. 9. Fig. 7 shows plotted dependence of pulse duration evolution along the train measured from single laser shot and recalculated. It can be seen that the pulse duration decreased from the initial 160 to 55 ps at the end of the train (Kubecek, 2010).

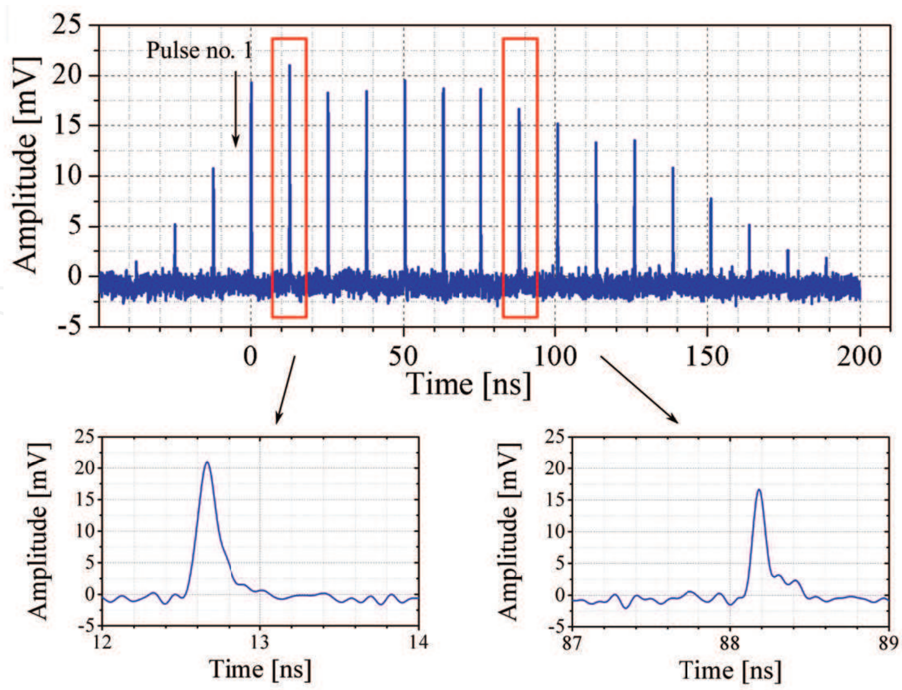

Fig. 6. Nd:GdVO$_4$ laser system output pulse train oscillogram (upper trace) and zoomed pulses no. 3 and 9 (lower traces).

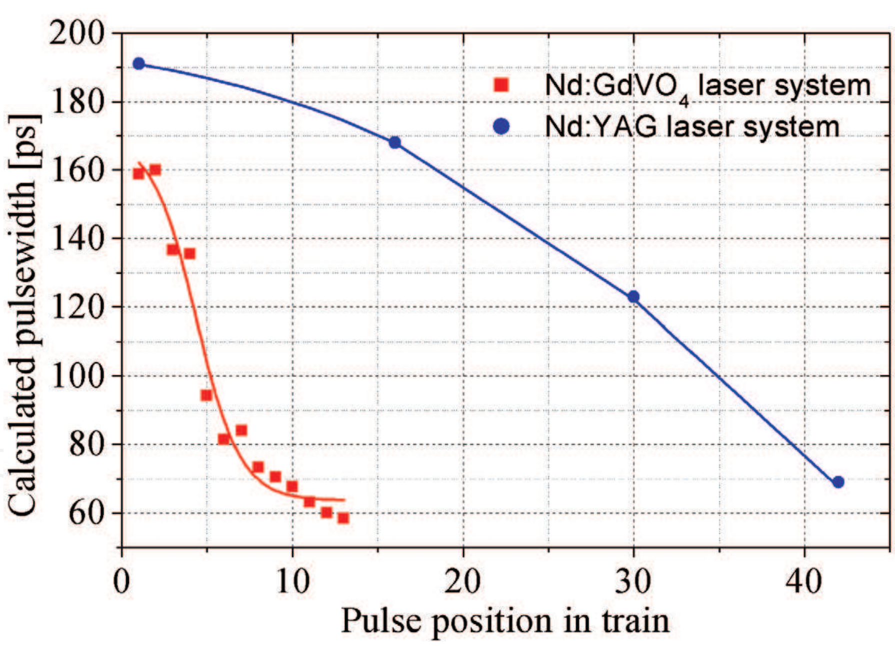

Fig. 7. Calculated pulse duration evolution along the trains generated by the Nd:GdVO$_4$ and Nd:YAG laser systems.

Similar pulse shortening effect was also observed in the output train of the passively mode-locked Nd:YAG laser with passive negative feedback when output trains containing hundred of pulses can be generated. Stretched 100 ns long pulse train shown in Fig. 8 has total energy of 60 μJ and contains $\sim$40 pulses. The pulse duration evolution along this train is shown in Fig. 7. The pulse shortening effect from original 190 ps in the beginning of the train to the final 70 ps was observed (Kubecek, 2009) resulting from the combined effect of the saturable absorber nonlinear transmission and passive negative feedback due to the beam defocusing via two-photon absorption in GaAs substrate of the semiconductor saturable absorber (Agnesi, 1992).

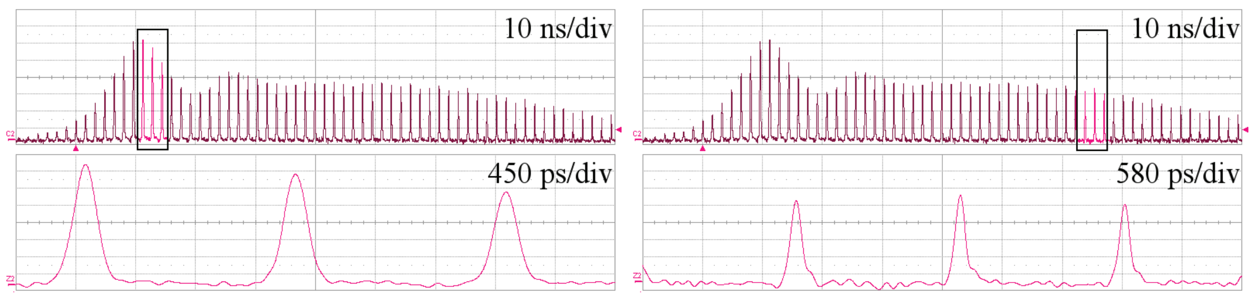

Fig. 8. Nd:YAG laser system output pulse train oscillogram (upper traces) and details of the pulse shapes from the beginning and end of the train (lower traces).

5. Conclusion

The aim of this chapter was the investigation of capabilities of the photodiode - oscilloscope measuring system for the single shot diagnostics of quasi-continuously pumped picosecond lasers. After the introduction, physics of light detection and photodiodes with emphasis on the response time of the PIN photodiodes was shortly discussed. In the third section, the oscilloscope - photodiode measuring system response and minimal pulse width was theoretically analyzed. According to this analysis, calculations based on datasheet values were performed for the used system consisting of the real time digital oscilloscope LeCroy SDA-9000 and PIN photodiode EOT ET-3500. The minimal pulse width (FWHM of the impulse response) of 50 ps was estimated. In the next section, this minimal pulse width was measured experimentally. Dependence of the width on different oscilloscope settings and waveform fitting was discussed. Measured minimal pulse width resulted in values between 60 and 63 ps and according to these results two calibration curves were obtained. In order to determine how short pulses can be reliably measured using the calibrated measuring system, pulses generated by two other laser sources were measured and their real widths were calculated and compared. It has been shown that even for pulses shorter than the minimal pulse width the useful real pulse width estimation can be obtained. Measurement and subsequent width calculation of the pulses with the duration comparable to the minimal pulse width can be performed with sufficient precision. The advantages of the calibrated measuring system were demostrated on the study of the laser pulse width stability and also on the investigation of the special effect - pulse shortening along the laser output pulse train.

6. Acknowledgements

The authors gratefully acknowledge the assistance of Pavel Honzatko, PhD and the consultations with David Vyhlidal.
This research has been supported by the Czech Science Foundation under grant No. 102/09/1741, the research projects of the Czech Ministry of Education MSM 6840770022

"Laser Systems, radiation and modern optical applications" and ME 10131 "Picosecond solid state lasers and parametric oscillators for sensors of rotation and other physical quantities."

7. References

Agilent. Evaluating oscilloscope bandwidths for your application. *Agilent Application note 1588*, URL: cp.literature.agilent.com/litweb/pdf/5989-5733EN.pdf.

Agnesi, A., et al. (1992). Generation of Extended Pulse Trains of Minimum Duration by Passive Negative Feedback Applied to Solid-state Q-Switched Lasers. *IEEE Journal of Quantum Electronics*, Vol. 28, No. 3, 710–719.

Andrews, J.R. (1989). TDR, step response and S parameter measurements in the time domain *Picosecond pulse labs - Application note AN-4*, URL: www.picosecond.com/objects/AN-04.pdf.

Berger, P.R. (1996). MSM Photodiodes *IEEE Potentials*, 25–29.

Bitter, M. (2000). *InP/InGaAs pin-Photodiode Arrays for Parallel Optical Interconnects*, Dissertation to the Swiss Federal Institute of Technology Zuerich, Switzerland.

Diels, J.-C. & Rudolph, W. (1995). *Ultrashort laser pulse phenomena*, Academic Press, ISBN 0-12-215492-4, USA.

Effenberger, F.J. & Joshi, A.M. (1996) Ultrafast, Dual-Depletion Region InGaAdInP p-i-n Detector. *Journal of lightwave technology*, Vol. 14, No. 8, 1859–1864.

Electro-Optics Technology, Inc. 10GHz GaAs and InGaAs Photodetectors datasheet, Jan 2011.

Gibbons, G. (1987). Gallium arsenide electronics. *Phys. Technol.*, Vol. 18, 5–16.

Ishibashi, T., et al. (2000). InP/InGaAs uni-traveling-carrier photodiodes. *IEICE Trans. Electron.*, Vol. E83-C, 938Ű-949.

Jelínek, M., et al. (2011). 0.8 mJ quasi-continuously pumped sub-nanosecond highly doped Nd:YAG oscillator-amplifier laser system in bounce geometry. *Laser Physics Letters*, Vol. 8, No. 3, 205–208.

Johnson, H.W. & Graham, M. (1993). *High Speed Digital Design: A Handbook of Black Magic*, Prentice Hall, ISBN 0133957241, USA.

Kache, S. (2005). *Optimization of charge collection efficiency in MSM photodetector.* Master thesis to University of Missouri-Columbia, USA.

Keller, U. (2002). *Ultrakurzzeit-Laserphysik*, Eidgenossische Technische Hochschule (ETH), Zurich, Switzerland.

Keller, U. (2007) Ultrafast solid-state lasers *Laser Physics and Applications, Subvolume B: Laser Systems.* Springer, ISBN 978-3-540-26033-2, Berlin, Germany.

Kubeček, V., et al. (2009). Pulse shortening by passive negative feedback in mode-locked train from highly-doped Nd:YAG in a bounce geometry. *Proc. SPIE*, Vol. 7354, 73540R.

Kubeček, V., et al. (2010). 0.4 mJ quasi-continuously pumped picosecond Nd:GdVO$_4$ laser with selectable pulse duration. *Laser Physics Letters*, Vol. 7, No. 2, 130–134.

Kubeček, V., et al. (2011). Cavity dumping of single 19 ps pulses from passively mode-locked quasi-continuously pumped highly doped Nd:YAG laser. *Proceedings of CLEO Europe*, Munich, Germany, May 2011.

LeCroy. Serial Data Analyzers (9 GHz - 18 GHz) datasheet, 2009.

Liu, K., et al. (2010). ZnO-Based Ultraviolet Photodetectors. *Sensors*, Vol. 10, 8604–8634, ISSN 1424-8220.

Malyshev, S. & Chizh, A. (2004). State of the art high-speed photodetectors for microwave photonics application. *Proc 15th Int. Conf. Microwaves, Radar and Wireless Communications*, Vol. 3, 765–775.

Nagatsuma, T. & Ito, H. (2011). High-Power RF Uni-Traveling-Carrier Photodiodes (UTC-PDs) and Their Applications. *Advances in photodiodes.* InTech, ISBN 978-953-307-163-3, Rijeka, Croatia.

Rulliere, C. (2003). *Femtosecond laser pulses*, Springer, ISBN 0-387-01769-0, USA.

Saleh, B.E.A. & Teich, M.C. (2007). *Fundamentals of photonics*, Wiley, ISBN 978-0-471-35832-9, USA.

Tektronix. XYZs of Oscilloscopes. *Tektronix Application note*, URL: www.tek.com.

Wang, J., at al. (2008). Evanescent-coupled Ge p-i-n photodetectors on Si-waveguide with SEG-Ge and comparative study of lateral and vertical p-i-n configurations. *IEEE Electron Device Letters*, Vol. 29, No. 5, 445–448.

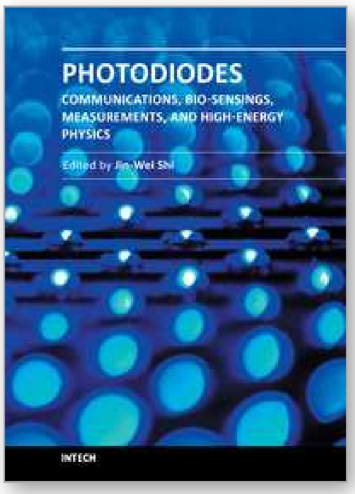

Photodiodes - Communications, Bio-Sensings, Measurements and High-Energy Physics

Edited by Associate Professor Jin-Wei Shi

ISBN 978-953-307-277-7
Hard cover, 284 pages
Publisher InTech
Published online 06, September, 2011
Published in print edition September, 2011

This book describes different kinds of photodiodes for applications in high-speed data communication, biomedical sensing, high-speed measurement, UV-light detection, and high energy physics. The photodiodes discussed are composed of several different semiconductor materials, such as InP, SiC, and Si, which cover an extremely wide optical wavelength regime ranging from infrared light to X-ray, making the suitable for diversified applications. Several interesting and unique topics were discussed including: the operation of high-speed photodiodes at low-temperature for super-conducting electronics, photodiodes for bio-medical imaging, single photon detection, photodiodes for the applications in nuclear physics, and for UV-light detection.

InTech Europe
University Campus STeP Ri
Slavka Krautzeka 83/A
51000 Rijeka, Croatia
Phone: +385 (51) 770 447
Fax: +385 (51) 686 166
www.intechopen.com

InTech China
Unit 405, Office Block, Hotel Equatorial Shanghai
No.65, Yan An Road (West), Shanghai, 200040, China
中国上海市延安西路65号上海国际贵都大饭店办公楼405单元
Phone: +86-21-62489820
Fax: +86-21-62489821